

# Self-Assembled Monolayers of $\omega$ -(3-Thienyl)alkanethiols on Gold

Heejoon Ahn, Myunghwan Kim, Daniel J. Sandman, and James E. Whitten\*

The Department of Chemistry and Center for Advanced Materials,  
The University of Massachusetts Lowell, Lowell, Massachusetts 01854-5047

Received November 7, 2002. In Final Form: February 24, 2003

Thiophene-containing alkanethiols, Th-(CH<sub>2</sub>)<sub>n</sub>-SH (Th = 3-thiophene) with  $n = 2, 6,$  and  $12,$  have been synthesized and self-assembled onto gold-coated Si(111) wafers. The properties of the monolayers have been compared with those of methyl-terminated self-assembled monolayers (SAMs) having the same number of methylene units. X-ray and ultraviolet photoelectron spectroscopies (XPS and UPS) demonstrate formation of surface thiolate bonds and assembly with the thiophene rings at the periphery of the monolayers. Dynamic contact angle measurements using water and hexadecane probe liquids are consistent with this conclusion and, particularly in the case of 12-(3-thienyl)dodecanethiol, indicate a densely packed, well-ordered monolayer. Ellipsometry measurements yield thickness values of 6.7, 10.7, and 17.9 Å for  $n = 2, 6,$  and  $12,$  respectively. Assuming the alkyl chains are in a fully extended all-trans conformation, these data indicate tilt angles of 42, 41, and 35°, respectively. Quartz crystal microbalance measurements demonstrate that the thienyl-terminated alkanethiol monolayers have similar packing densities compared to methyl-terminated SAMs of similar lengths. Thermal stability measurements using XPS and UPS show that the thienyl-terminated SAMs are stable to at least 100 °C but desorb/decompose on heating to 150 °C.

## Introduction

Langmuir–Blodgett (LB) and self-assembly techniques are the most common methods for forming ultrathin organic films. Physisorbed films may be produced by the LB method by passing a solid substrate through the liquid/air interface of an aqueous solution containing an organic monolayer film. When the substrate moves through the interface, organic molecules are transferred onto the solid substrate.<sup>1</sup> Self-assembled monolayers (SAMs) are molecular assemblies that are based on monomolecular adsorption and arrangement between the liquid and solid phases. These are also referred to as “programmed assemblies”.<sup>2</sup> The origin of SAMs can be traced to the work of Zisman et al.<sup>3</sup> who formed well-oriented and nearly close-packed monolayer films by immersing glass into *n*-eicosyl alcohol, primary *n*-octadecylamine, and *n*-nonadecanoic acid solutions. These films exhibited wetting properties similar to those of LB films. Interest in SAMs increased tremendously after the discovery of the formation of alkanethiolates on gold by Nuzzo and Allara.<sup>4</sup> Other types of SAMs on a variety of substrates have since been reported, but among these systems, those made by adsorbing alkanethiols on gold surfaces have been the most widely studied because of their ease of preparation, range of functionalities, and excellent stabilities.<sup>5,6</sup> SAMs potentially have a wide range of applications, including

corrosion protection,<sup>7</sup> nanolithography,<sup>8</sup> and molecular electronics.<sup>9</sup>

Alkanethiol adsorbates with long alkyl chains (>C<sub>10</sub>) tend to form highly ordered, oriented monolayer films tilted 20–30° from the surface normal. However, for short alkyl chains (<C<sub>6</sub>), less ordered monolayers with lower packing densities are generally observed.<sup>6,10</sup> These observations demonstrate the importance of van der Waals and electrostatic interactions between the alkyl chains in the assembled monolayers. Surface properties such as wetting,<sup>6,11</sup> friction,<sup>12,13</sup> adhesion,<sup>14</sup> and adsorption<sup>15</sup> can be controlled by tailoring the exposed surface of the monolayer by judicious selection of tail group.

SAMs containing aromatic tail groups such as pyrrole,<sup>16–19</sup> aniline,<sup>20</sup> benzene,<sup>21</sup> and thiophene<sup>21–25</sup> are attractive because of the possibilities that they can be

\* Corresponding author. Fax: (978)934-3013. Phone: (978)934-3666. E-mail: James\_Whitten@uml.edu.

(1) Ulman, A. *An Introduction to Ultrathin Organic Films: From Langmuir–Blodgett to Self-Assembly*; Academic Press: New York, 1991; pp 101–132.

(2) Lehn, J.-M. *Supramolecular Chemistry*; VCH: Weinheim, 1995; pp 139–144.

(3) Bigelow, W. C.; Pickett, D. L.; Zisman, W. A. *J. Colloid Sci.* **1946**, *1*, 513.

(4) Nuzzo, R. G.; Allara, D. L. *J. Am. Chem. Soc.* **1983**, *105*, 4481.

(5) Ulman, A. *An Introduction to Ultrathin Organic Films: From Langmuir–Blodgett to Self-Assembly*; Academic Press: New York, 1991; pp 279–281 and references therein.

(6) Bain, C. D.; Troughton, E. B.; Tao, Y.-T.; Evall, J.; Whitesides, G. M.; Nuzzo, R. G. *J. Am. Chem. Soc.* **1989**, *111*, 321.

(7) Jennings, G. K.; Munro, J. C.; Yong, T.-H.; Laibinis, P. E. *Langmuir* **1998**, *14*, 6130.

(8) Whitesides, G. M.; Love, J. C. *Sci. Am.* **2001**, *285*, 39.

(9) Donhauser, Z. J.; Mantoosh, B. A.; Kelly, K. F.; Bumm, L. A.; Monnell, J. D.; Stapleton, J. J.; Price, D. W., Jr.; Rawlett, A. M.; Allara, D. L.; Tour, J. M.; Weiss, P. S. *Science* **2001**, *292*, 2303.

(10) Porter, M. D.; Bright, T. B.; Allara, D. L.; Chidsey, C. E. D. *J. Am. Chem. Soc.* **1987**, *109*, 3559.

(11) Laibinis, P. E.; Whitesides, G. M. *J. Am. Chem. Soc.* **1992**, *114*, 1990.

(12) Green, J.-B. D.; McDermott, M. T.; Porter, M. D.; Siperko, L. M. *J. Phys. Chem.* **1995**, *99*, 10960.

(13) Lee, S.; Puck, A.; Graupe, M.; Colorado, R., Jr.; Shon, Y.-S.; Lee, T. R.; Perry, S. S. *Langmuir* **2001**, *17*, 7364.

(14) Ulman, A.; Tillman, N. *Langmuir* **1989**, *5*, 1418.

(15) Prime, K. L.; Whitesides, G. M. *J. Am. Chem. Soc.* **1993**, *115*, 10714.

(16) Willcutt, R. J.; McCarley, R. L. *J. Am. Chem. Soc.* **1994**, *116*, 10823.

(17) Willcutt, R. J.; McCarley, R. L. *Langmuir* **1995**, *11*, 296.

(18) Sayre, C. N.; Collard, D. M. *Langmuir* **1995**, *11*, 302.

(19) Simon, R. A.; Ricco, A. J.; Wrighton, M. S. *J. Am. Chem. Soc.* **1982**, *104*, 2031.

(20) Kuwabata, S.; Fukuzaki, R.; Nishizawa, M.; Martin, C. R.; Yoneyama, H. *Langmuir* **1999**, *15*, 6807.

(21) Nakamura, T.; Kondoh, H.; Matsumoto, M.; Nozoye, H. *Langmuir* **1996**, *12*, 5977.

(22) Sullivan, J. T.; Harrison, K. E.; Mizzell, J. P., III; Kilbey, S. M., II *Langmuir* **2000**, *16*, 9797.

polymerized by chemically or electrochemically oxidizing the aromatic functional group. Electrochemically polymerized pyrrolyl-alkanethiol SAMs<sup>16,17</sup> and their aniline analogues<sup>20</sup> exhibit enhanced stability against reductive desorption compared to the corresponding monolayers prior to electrooxidative polymerization.

Pyrrole,<sup>26</sup> furan,<sup>27</sup> benzene,<sup>28</sup> and thiophene<sup>26,29–31</sup> cryogenically condensed onto conducting substrates may be polymerized/oligomerized by X-ray or electron irradiation. Recently, we reported that Mg K $\alpha$  X-ray and electron irradiation of 3-hexylthiophene condensed on gold results in the formation of oligomeric films, with clear retention of conjugation evidenced by valence photoelectron spectroscopy.<sup>32</sup> We also demonstrated that the oligomerized 3-hexylthiophene film is fluorescent,<sup>33</sup> and possibilities exist for nanolithographically forming conjugated oligomers by this method.

Recent studies indicate that thiophene itself may self-assemble on gold.<sup>34,35</sup> Motivated by the possibility of polymerizing/oligomerizing thiophene-containing SAMs and an interest in determining how the thiophene tail groups affect the nature of the assembly, we have initiated a study of the self-assembly of  $\omega$ -(3-thienyl)alkanethiols, Th-(CH<sub>2</sub>)<sub>*n*</sub>-SH with *n* = 2, 6, and 12, onto Au(111) surfaces. Note that this is the first report of the synthesis and self-assembly of these molecules. The nature of the SAMs has been studied with a variety of techniques including ellipsometry, contact angle measurements, quartz crystal microbalance (QCM) measurements, X-ray photoelectron spectroscopy (XPS), and ultraviolet photoelectron spectroscopy (UPS). The latter technique is particularly useful for this system since it allows the valence electronic spectra of conjugated molecules to be measured. Thermal stability of the 12-(3-thienyl)alkanethiols on gold has also been determined by XPS and UPS.

## Experimental Section

**Materials.** Thienyl-terminated alkanethiols, Th-(CH<sub>2</sub>)<sub>*n*</sub>-SH (Th = 3-thiophene) with *n* = 2, 6, and 12, have been synthesized. The chemical structures of these compounds are illustrated in Figure 1. All chemicals used in the syntheses described below and the Me-(CH<sub>2</sub>)<sub>*n*</sub>-SH (Me = methyl) with *n* = 2, 6, and 12 used for comparative studies were purchased from Aldrich and used as received.

**Synthesis of 12-(3-Thienyl)dodecanethiol.** The synthetic scheme of 12-(3-thienyl)dodecanethiol from *p*-methoxyphenol is shown in Figure 2. Briefly, *p*-methoxyphenoxydodecyl bromide was prepared from the reaction of *p*-methoxyphenol and 1,12-dibromododecane.<sup>36</sup> This compound was reacted with magnesium to form its Grignard reagent, which was then coupled with

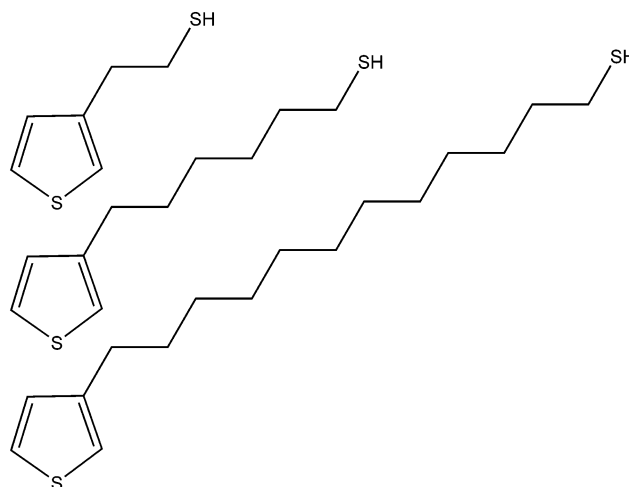


**Figure 1.** Chemical structures of thienyl-terminated alkanethiols.

3-bromothiophene in the presence of nickel phosphine ([1,3-bis-(diphenylphosphino)propane]dichloronickel(II)), as a catalyst, in refluxing tetrahydrofuran. 3-(12-*p*-Methoxyphenoxydodecyl)-thiophene was then reacted with the mixture of hydrogen bromide and acetic anhydride.<sup>37</sup> 3-(12-Bromododecyl)thiophene and thiourea were mixed in ethanol and refluxed under a stream of nitrogen overnight. Sodium hydroxide solution was added and further refluxed for 6 h under an inert atmosphere. Ethanol was removed by rotary evaporation, and the residual oil was neutralized with dilute sulfuric acid. The organic layer was obtained by washing the aqueous layer with ether, and the residue was dissolved in petroleum ether. A silica-gel-packed column was used to separate the desired 12-(3-thienyl)dodecanethiol from side products. The product was characterized by Fourier transform infrared (FTIR) spectroscopy and <sup>1</sup>H and <sup>13</sup>C NMR, as follows.

**12-(3-Thienyl)dodecanethiol** (Th-(CH<sub>2</sub>)<sub>12</sub>-SH). FTIR (neat): 770, 834, 858, 880, 1080, 1152, 1260, 1440, 1464, 1537, 2567 (-SH), 2853, 2925, 3050, 3104 cm<sup>-1</sup>. <sup>1</sup>H NMR (250 MHz, CDCl<sub>3</sub>)  $\delta$ : 7.23 (m, 1H, ArH), 6.95 (s, 1H, ArH), 6.93 (s, 1H, ArH), 2.63 (t, *J* 7.5, 2H, -CH<sub>2</sub>-Ar), 2.53 (t, *J* 7.7, 2H, -CH<sub>2</sub>-S), 1.62 (m, 4H, -CH<sub>2</sub>-), 1.35 (m, 17H, -CH<sub>2</sub>-, -SH). <sup>13</sup>C NMR (200 MHz, CDCl<sub>3</sub>)  $\delta$ : 143.21, 128.25, 124.99, 119.71, 34.02, 30.53, 30.25, 29.88, 29.54 (2C), 29.48, 29.43, 29.30, 29.04, 28.35, 24.63.

**Synthesis of 2-(3-Thienyl)ethanethiol and 6-(3-Thienyl)hexanethiol.** 3-(2-Bromoethyl)thiophene and 3-(6-bromohexyl)-thiophene were synthesized and purified as described in the literature.<sup>36–38</sup> These were reacted with thiourea in refluxing ethanol under an inert atmosphere, yielding 2-(3-thienyl)-ethanethiol and 6-(3-thienyl)hexanethiol, respectively. The desired products were purified via the same method as described above for 12-(3-thienyl)dodecanethiol and characterized by FTIR spectroscopy and <sup>1</sup>H and <sup>13</sup>C NMR, as follows.

**2-(3-Thienyl)ethanethiol** (Th-(CH<sub>2</sub>)<sub>2</sub>-SH). FTIR (neat): 790, 831, 855, 1080, 1152, 1240, 1290, 1410, 1430, 1530, 2560 (-SH), 2850, 2930, 2960, 3050, 3100 cm<sup>-1</sup>. <sup>1</sup>H NMR (200 MHz, CDCl<sub>3</sub>)  $\delta$ : 7.27 (m, 1H, ArH), 7.02 (m, 1H, ArH), 6.95 (m, 1H, ArH), 2.94 (t, *J* 5, 2H, -CH<sub>2</sub>Ar), 2.8 (m, 2H, -CH<sub>2</sub>SH), 1.42 (t, *J* 7.7, 1H, -SH). <sup>13</sup>C NMR (200 MHz, CDCl<sub>3</sub>)  $\delta$ : 140.06, 127.85, 125.66, 121.32, 34.60, 25.37.

**6-(3-Thienyl)hexanethiol** (Th-(CH<sub>2</sub>)<sub>6</sub>-SH). FTIR (neat): 770, 834, 858, 880, 1080, 1152, 1260, 1460, 1480, 1560, 2580 (-SH), 2870, 2950, 3060, 3120 cm<sup>-1</sup>. <sup>1</sup>H NMR (250 MHz, CDCl<sub>3</sub>)  $\delta$ : 7.23 (m, 1H, ArH), 6.94 (s, 1H, ArH), 6.92 (s, 1H, ArH), 2.63 (t, *J* 7.5, 2H, -CH<sub>2</sub>-Ar), 2.53 (t, *J* 7.7, 2H, -CH<sub>2</sub>-S), 1.60 (m, 4H, -CH<sub>2</sub>-), 1.38 (m, 5H, -CH<sub>2</sub>-, -SH). <sup>13</sup>C NMR (250 MHz, CDCl<sub>3</sub>)  $\delta$ : 142.93, 128.19, 125.10, 119.82, 33.90, 30.36, 30.13, 28.67, 28.12, 24.58.

(36) Ashley, J. N.; Collins, R. F.; Davis, M.; Sirett, N. E. *J. Chem. Soc.* **1958**, 3303.

(37) Bäuerle, P.; Würthner, F.; Heid, S. *Angew. Chem. Int. Ed. Engl.* **1990**, 29, 419.

(38) Hong, X.; Tyson, J. C.; Middlecoff, J. S.; Collard, D. M. *Macromolecules* **1999**, 32, 4232.

(23) Ito, E.; Yamamoto, M.; Kajikawa, K.; Yamashita, D.; Ishii, H.; Ouchi, Y.; Seki, K. *Langmuir* **2001**, 17, 4282.

(24) Okawa, H.; Wada, T.; Sasabe, H.; Kajikawa, K.; Seki, K.; Ouchi, Y. *Jpn. J. Appl. Phys.* **2000**, 39, 252.

(25) Appelhans, D.; Ferse, D.; Adler, H.-J. P.; Plieth, W.; Fikus, A.; Grundke, K.; Schmitt, F.-J.; Bayer, T.; Adolph, B. *Colloids Surf., A* **2000**, 161, 203.

(26) Salaneck, W. R.; Erlandsson, R.; Prejza, J.; Lundstrom, I.; Inganas, O. *Synth. Met.* **1993**, 5, 125.

(27) Qiao, M. H.; Yan, F. Q.; Sim, W. S.; Deng, J. F.; Xu, G. Q. *Surf. Sci.* **2000**, 460, 67.

(28) Whitten, J. E.; Gomer, R. *Surf. Sci.* **1996**, 347, 280.

(29) Salaneck, W. R.; Wu, C. R.; Nilsson, J. O.; Brédas, J.-L. *Synth. Met.* **1987**, 21, 57.

(30) Land, T. A.; Hemminger, J. C. *Surf. Sci.* **1992**, 268, 179.

(31) Raza, H.; Wincott, P. L.; Thornton, G.; Casanova, R.; Rodriguez, A. *Surf. Sci.* **1997**, 390, 256.

(32) Hernandez, J. E.; Ahn, H.; Whitten, J. E. *J. Phys. Chem. B* **2001**, 105, 8339.

(33) Ahn, H.; Whitten, J. E. *J. Phys. Chem. B* **2002**, 106, 11404.

(34) Dishner, M. H.; Hemminger, J. C.; Feher, F. J. *Langmuir* **1996**, 12, 6176.

(35) Noh, J.; Ito, E.; Nakajima, K.; Kim, J.; Lee, H.; Hara, M. *J. Phys. Chem. B* **2002**, 106, 7139.

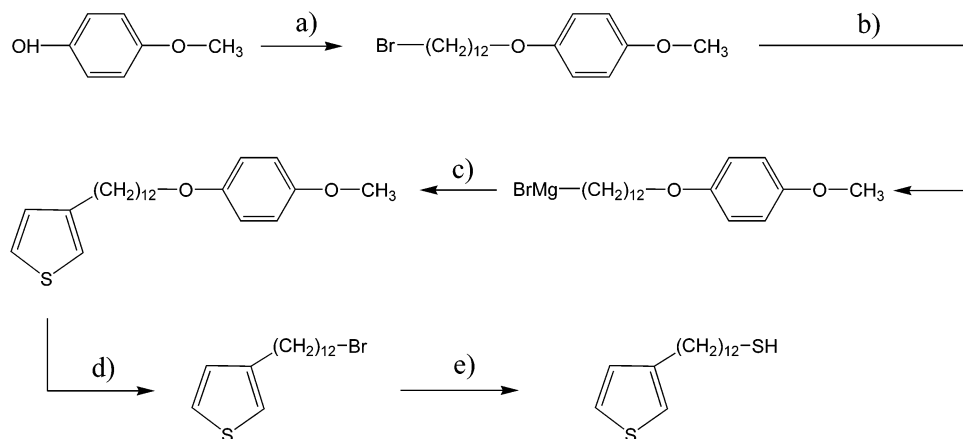


**Figure 2.** Synthesis of 12-(3-thienyl)dodecanethiol: (a)  $\text{Br}(\text{CH}_2)_{12}\text{Br}/\text{KOH}/\text{MeOH}$ , (b)  $\text{Mg}/\text{THF}$ , (c)  $\text{NiDPPPCl}_2/\text{C}_4\text{H}_3\text{SBr}$ , (d)  $\text{HBr}/\text{Ac}_2\text{O}$ , and (e)  $(\text{NH}_2)_2\text{CS}/\text{NaOH}$ .

**Substrate Preparation.** The gold substrates were prepared by thermal deposition in a ca.  $5 \times 10^{-7}$  mbar vacuum, from a tungsten filament that had been wrapped with 99.999% gold wire, onto polished Si(111) wafers that had been ultrasonicated in methanol and acetone and dried prior to use. The gold deposition was performed with the substrates at room temperature. No interfacial Cr or Ti layers were used between the silicon and gold. X-ray diffraction showed that the evaporated gold films were predominantly Au(111). The areas of the Si(111) wafers were ca.  $1 \text{ cm}^2$ , and the gold thickness was approximately 2000 Å. To minimize contamination, the gold-covered substrates were immersed in the thiol solutions immediately after removal from the vacuum.

**SAM Preparation.** SAMs of thienyl- and methyl-terminated alkanethiols were formed by immersion of freshly prepared gold substrates in 1.0 mM thiol solutions in chloroform for  $\sim 24$  h at room temperature. The SAMs were removed from the thiol solutions, rinsed carefully with chloroform, and dried in a nitrogen stream just prior to the particular characterization experiment.

**Photoelectron Spectroscopy.** XPS and UPS measurements were performed in a VG ESCALAB MK II photoelectron spectrometer equipped with a Mg K $\alpha$  X-ray source ( $h\nu = 1253.6$  eV) and a He I ultraviolet lamp ( $h\nu = 21.2$  eV). The base pressure was about  $1 \times 10^{-9}$  mbar. Electron kinetic energies were measured by a concentric hemispherical analyzer operating in constant pass energy mode and detected approximately normal to the sample plane unless otherwise stated. In some cases, to obtain information about the orientation of the thienyl-terminated SAMs, XPS was performed at takeoff angles (i.e., the angle between the surface of the sample and the photoelectron detector) of  $15^\circ$ ,  $60^\circ$ , and  $90^\circ$ . Peak fitting of the X-ray photoelectron S 2p spectra was carried out with a Shirley type background and 20% Lorentzian/80% Gaussian components. The S  $2p_{3/2}$  and S  $2p_{1/2}$  doublets were fitted using a fixed spin-orbit splitting value of 1.2 eV and intensity ratio of 2:1 S  $2p_{3/2}/\text{S } 2p_{1/2}$ .<sup>39,40</sup> The binding energy scale is referenced to the Fermi level for both XPS and UPS. To prevent charging during the experiments, silver paint was used to make electrical contact from the edges of the gold-coated Si(111) wafers to the sample stubs. The sample stubs were held at electrical ground during the XPS measurements and at  $-6.1$  V during UPS. In the latter case, the negative bias was necessary in order to be able to measure the entire width of the spectrum. This voltage was accounted for in converting the measured kinetic energies to binding energies.

**Ellipsometric Measurements.** The thickness of the SAMs was measured using a Rudolph Research AutoEL-III ellipsometer equipped with a 632.8 nm He-Ne laser at an incident angle of  $70^\circ$ . To obtain accurate optical constants of a bare gold surface, the gold substrate was oxygen plasma cleaned for 30 s just prior to ellipsometric baseline measurement. The value reported is

the average of five separate data points. A refractive index of 1.45 was assumed for the thienyl-terminated alkanethiol SAMs, and the variation of measured thickness was  $\pm 1$  Å.

**Contact Angle Measurements.** Dynamic advancing and receding contact angles were measured using a KSV Sigma 70 dynamic contact angle analyzer (KSV Instruments LTD). The dynamic contact angle measurement was based on the Wilhelmy plate method given by the following equation:<sup>41</sup>

$$F_w = P\gamma \cos \theta \quad (1)$$

where  $F_w$  is the wetting force,  $P$  is the wetted perimeter of the sample,  $\gamma$  is the surface tension of the liquid, and  $\theta$  is the contact angle between the liquid and the sample. The wetting force is experimentally determined, and using known values of  $P$  and  $\gamma$ ,  $\theta$  can be calculated using eq 1. For dynamic contact angle measurements, SAMs were formed on double-sided gold-coated Si(111) wafers. The SAMs were immersed in and drawn out of contact angle liquids at a rate of 1 mm/min to obtain the wetting force as a function of immersion depth. Each contact angle measurement was repeated three times.

**Quartz Crystal Microbalance Measurement.** The QCM devices (International Crystal Manufacturing) consisted of double-sided 5 MHz AT-cut quartz crystals with 1000 Å thermally deposited gold electrodes having a diameter of 0.268 in. A typical experimental sequence was as follows. A QCM was dipped in piranha solution (1:3  $\text{H}_2\text{O}_2$  (30%)/ $\text{H}_2\text{SO}_4$ ) for 5 min and ultrasonicated in deionized water for 1 min. The cleaned QCM was then rinsed with anhydrous ethanol and dried in a stream of pure nitrogen. It was then immediately immersed in pure chloroform and allowed to dry to obtain a baseline frequency reading. Ex situ QCM adsorption measurements were performed by immersing the crystal in a 1 mM thiol solution for a measured length of time, washing the crystal in pure chloroform for 1 min, and allowing the crystal to dry prior to recording the frequency. The packing density of molecules on the gold electrode surface was calculated from the frequency change using the following equation:<sup>42</sup>

$$\text{packing density (molecules/cm}^2\text{)} = \frac{\Delta\nu \rho_g N_q \times 6.02 \times 10^{23}}{-\nu_0^2 M_w} \quad (2)$$

where  $\Delta\nu$  is half of the frequency change in hertz (since both sides of the QCM were used),  $\rho_g$  is the density of LiF ( $2.648 \text{ g cm}^{-3}$ ),  $N_q$  is the frequency constant for an AT-cut quartz ( $1.668 \times 10^5 \text{ Hz cm}^2$ ),  $\nu_0$  is the nominal frequency of the quartz crystal, and  $M_w$  is the molecular weight of the adsorbate (g/mol).

**Thermal Stability Measurements.** To measure the thermal stability of the SAMs, the monolayer-covered Au/Si(111) substrates were heated in a  $10^{-9}$  mbar vacuum in the sample

(39) Wagner, C. D.; Riggs, W. M.; Davis, L. E.; Moulder, J. F.; Muilenberg, G. E. *Handbook of X-ray Photoelectron Spectroscopy*; Perkin-Elmer Corp.: Eden Prairie, MN, 1979.

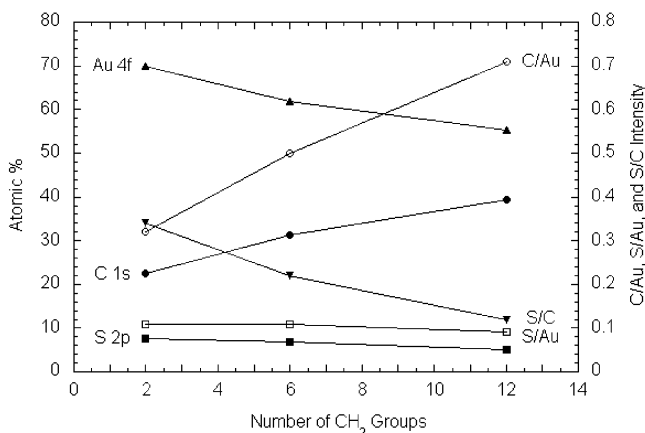
(40) Briggs, D. *Surface Analysis of Polymers by XPS and Static SIMS*; Cambridge University Press: Cambridge, U.K., 1998; pp 34–39.

(41) Adamson, A. W.; Gast, A. P. *Physical Chemistry of Surfaces*, 6th ed.; Wiley-Interscience: New York, 1997; pp 23–26.

(42) Sauerbrey, G. *Z. Phys. (Munich)* **1959**, *155*, 206.

**Table 1. Atomic Percentages of Elements or Atomic Ratios for Thienyl-Terminated Alkanethiol SAMs on Au/Si(111) as a Function of Takeoff Angles**

atomic % or atomic ratios	Th-(CH <sub>2</sub> ) <sub>2</sub> -SH			Th-(CH <sub>2</sub> ) <sub>6</sub> -SH			Th-(CH <sub>2</sub> ) <sub>12</sub> -SH		
	15°	60°	90°	15°	60°	90°	15°	60°	90°
C	51.0	26.1	22.4	53.9	34.7	31.2	69.7	51.4	39.5
S	13.7	8.0	7.6	11.1	7.4	6.9	10.3	7.4	5.1
Au	35.3	65.9	70.0	35.0	57.9	61.9	20.0	41.2	55.4
S/Au	0.39	0.12	0.11	0.21	0.13	0.11	0.51	0.18	0.09
C/Au	1.44	0.40	0.32	1.54	0.60	0.50	3.48	1.25	0.71
S/C	0.27	0.31	0.34	0.21	0.21	0.22	0.15	0.14	0.13
S (thiophene)/S (thiol)	1.29	1.27	1.16	1.29	0.65	0.89	1.96	1.94	1.11
S (thiophene)/Au	0.21	0.07	0.06	0.18	0.05	0.05	0.33	0.12	0.05

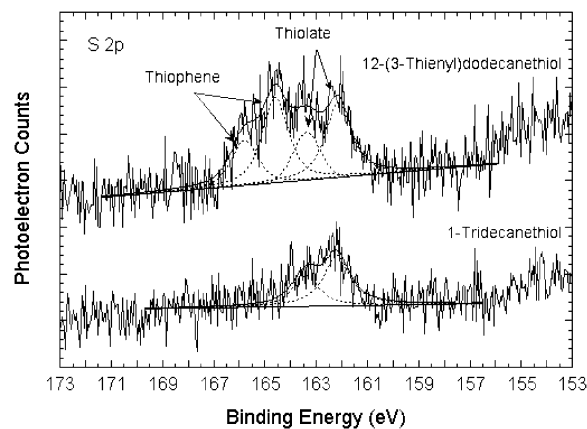
**Figure 3.** Atomic percentages of C (●), S (■), and Au (▲) and the ratios of C/Au (○), S/Au (□), and S/C (▼) as a function of methylene chain length for thienyl-terminated alkanethiol SAMs on Au/Si(111). Atomic percentages and ratios were derived from integration of the C 1s, S 2p, and Au 4f XPS peaks at a takeoff angle of 90°.

preparation chamber of the photoelectron spectrometer. A commercial sample heater (VG model 240) was used into which a carousel holding multiple samples could be inserted. A thermocouple was attached to the carousel to monitor the temperature. The sample was heated at the specified temperature for 30 min prior to performing the photoelectron spectroscopy experiments, which were carried out at ambient temperature.

## Results and Discussion

**Photoelectron Spectroscopy.** XPS has been used to verify the formation of monolayers of thienyl-terminated alkanethiols on Au(111) substrates. Table 1 shows the atomic ratios of thienyl-terminated alkanethiol SAMs derived from integration of the C 1s, S 2p, and Au 4f peaks, with correction for their sensitivity factors.<sup>43</sup> The theoretical ratios of S/C for Th-(CH<sub>2</sub>)<sub>n</sub>-SH are 0.33, 0.20, and 0.12 for  $n = 2, 6,$  and  $12,$  respectively. The observed S/C ratios at a 90° takeoff angle are in reasonable agreement with the theoretical values. Figure 3 shows a graph of atomic percentages and atomic ratios, as determined by XPS, as a function of the number of methylene units. The C/Au ratio increases, the S/C ratio decreases, and the S/Au ratio changes only slightly with increasing chain length. These observations confirm the adsorption of the three thienyl-terminated alkanethiols on the gold substrates.

Figure 4 presents the S 2p XPS spectrum of 12-(3-thienyl)dodecanethiol on Au(111). For comparison, corresponding data for 1-tridecanethiol, a methyl-terminated alkanethiol with the same number of methylene units, are also included. The situation is complicated by spin-orbit coupling that leads to two peaks for each of the two different types of sulfurs (i.e., thiol vs thiophene). Using

**Figure 4.** Mg K $\alpha$  XPS of the S 2p region of self-assembled 12-(3-thienyl)dodecanethiol and 1-tridecanethiol monolayers on Au/Si(111) at a takeoff angle of 90°.

expected peak binding energies,<sup>44–50</sup> the peak fits were constrained at maximum intensity binding energies of 162.1, 163.3, 164.6, and 165.8 eV. A full width at half-maximum (fwhm) of 1.23 eV was used based on measurements in the same photoelectron spectrometer of the 1-tridecanethiol monolayer and a regioregular poly(3-hexylthiophene) film. The agreement of the fit to the experimental data confirms that the 12-(3-thienyl)dodecanethiol monolayer is composed of two sets of spin-orbit coupled S 2p doublets from the thiol and thiophene sulfur species. The lower binding energy peaks at 162.1 and 163.3 eV may be assigned to thiols chemisorbed on the Au surface, indicating thiolate formation.<sup>44–48</sup> The higher binding energy peaks at 164.6 and 165.8 eV are due to the thiophene sulfur atoms.<sup>49,50</sup> These results are consistent with 12-(3-thienyl)dodecanethiol bonding to gold via the thiol sulfur.

XPS at various takeoff angles has also been performed. Sampling depth is related to the takeoff angle by the following equation:

$$d_s = 3\lambda_{AL} \sin \theta \quad (3)$$

where  $d_s$  is the XPS sampling depth,  $\lambda_{AL}$  is the attenuation

(44) Laibinis, P. E.; Whitesides, G. M.; Allara, D. L.; Tao, Y.-T.; Parikh, A. N.; Nuzzo, R. G. *J. Am. Chem. Soc.* **1991**, *113*, 7152.

(45) Heister, K.; Zharnikov, M.; Grunze, M.; Johansson, L. S. O. *J. Phys. Chem. B* **2001**, *105*, 4058.

(46) Bain, C. D.; Biebuyck, H. A.; Whitesides, G. M. *Langmuir* **1989**, *5*, 723.

(47) Evans, S. D.; Goppert-Berarducci, K. E.; Urankar, E.; Gerenser, L. J.; Ulman, A.; Snyder, R. G. *Langmuir* **1991**, *7*, 2700.

(48) Castner, D. G.; Hinds, K.; Grainger, D. W. *Langmuir* **1996**, *12*, 5083.

(49) Dannetun, P.; Boman, M.; Stafström, S.; Salaneck, W. R.; Lazzaroni, R.; Fredriksson, C.; Brédas, J.-L.; Zamboni, R.; Taliani, C. *J. Chem. Phys.* **1993**, *99*, 664.

(50) Fahlman, M.; Birgersson, J.; Kaeriyama, K.; Salaneck, W. R. *Synth. Met.* **1995**, *75*, 223.

(43) Skofield, J. H. *J. Electron Spectrosc.* **1976**, *8*, 129.

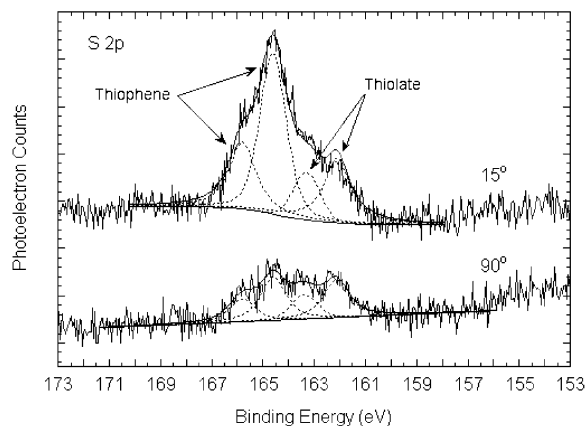


**Figure 5.** Mg K $\alpha$  XPS of the S 2p region of self-assembled 12-(3-thienyl)dodecanethiol monolayers on Au/Si(111) at takeoff angles of 90° and 15°.

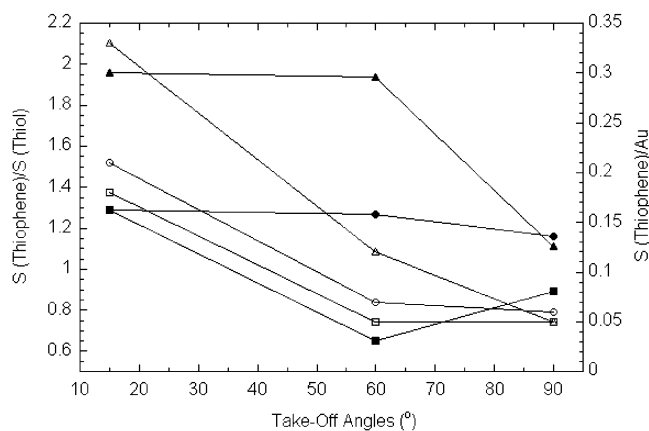


**Figure 6.** Area ratios of S (thiophene)/S (thiol) and S (thiophene)/Au as a function of takeoff angles for 2-(3-thienyl)ethanethiol (● and ○), 6-(3-thienyl)hexanethiol (■ and □), and 12-(3-thienyl)dodecanethiol (▲ and △) SAMs on Au/Si(111). All filled symbols correspond to S (thiophene)/S (thiol), and all empty symbols correspond to S (thiophene)/Au.

length of the measured electrons, and  $\theta$  is the electron takeoff angle relative to the surface plane.<sup>40</sup> As the takeoff angle decreases, sampling depth also decreases, and surface sensitivity increases.<sup>39</sup> Figure 5 displays the results of XPS S 2p spectra for 12-(3-thienyl)dodecanethiol monolayers at takeoff angles of 90° and 15°. Peak fitting has been used to compute the area ratios of S 2p (thiophene) to S 2p (thiol). As the takeoff angle decreases from 90° to 15°, the relative areas of the S 2p (thiophene) peaks increase. As shown in Table 1, the intensity ratios of S 2p (thiophene)/S 2p (thiol) at takeoff angles of 90° and 15° are 1.11 and 1.96, respectively. This indicates that the thiophene sulfur atoms are nearer to the sample outer surface than the thiol sulfurs. Figure 6 displays the corresponding data. We observe 11.2%, 44.9%, and 76.6% increases in the ratios of S 2p (thiophene)/S 2p (thiol) for Th-(CH<sub>2</sub>)<sub>n</sub>-SH monolayers with  $n = 2, 6,$  and  $12,$  respectively, as the takeoff angle decreases from 90° to 15°. This is, again, consistent with the thiophene rings being at the outer periphery of the assembly.

Because of the limited escape depths of photoelectrons, the intensity of photoelectrons from the gold substrate is inversely related to the thickness of adsorbed monolayers. Laibinis et al.<sup>44</sup> observed a regular decrease in photoelectron intensity due to the underlying gold substrates as the number of methylene units in the  $n$ -alkanethiols increased. We observe similar decreases in the intensity of the Au 4f peak for the thienyl-terminated alkanethiol

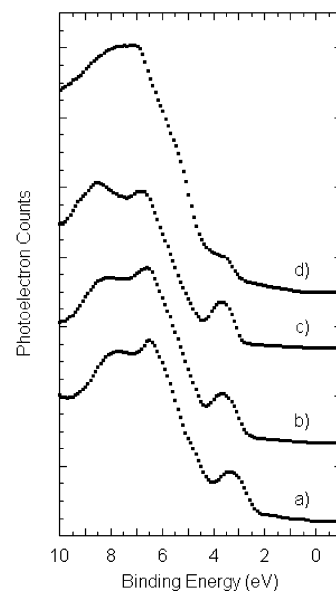


**Figure 7.** He I UPS of self-assembled (a) 2-(3-thienyl)ethanethiol, (b) 6-(3-thienyl)hexanethiol, (c) 12-(3-thienyl)dodecanethiol, and (d) 1-tridecanethiol monolayers on Au/Si(111).

monolayers as chain length increases. The relative areas of the Au 4f peaks for the  $\omega$ -thienyl alkanethiols can be calculated from Table 1 and are 1.0, 1.1, and 1.3 for methylene unit lengths of 12, 6, and 2, respectively. This indicates that the longer thienyl-terminated alkanethiols form thicker monolayers on gold substrates.

UPS has been used to study the valence electronic structure of the thienyl-terminated alkanethiol monolayers on gold. Figure 7 depicts UPS spectra of  $\omega$ -(3-thienyl)alkanethiols and 1-tridecanethiol SAMs on gold substrates. To assign the UPS peaks, we have calculated the ionization potentials of gas-phase thienyl- and methyl-terminated alkanethiol molecules using Gaussian 98. A restricted Hartree-Fock Outer-Valence Green's Function (ROVGF) calculation of ionization potentials has been performed with a STO-3G basis set; geometry optimization was carried out at the 6-31G level. For 12-(3-thienyl)dodecanethiol monolayers, the peak in the vicinity of 3.8 eV is attributable to localized electronic states with strong contributions from thiophene ring sulfur atoms and sulfur atoms in the thiol groups. The peaks at 6.6 and 8.5 eV are due to the nonbonding orbitals of sulfur atoms and some  $\sigma$  orbitals in the alkyl chains. In the case of 1-tridecanethiol SAMs, the feature at 3.5 eV is due to the highest occupied molecular orbitals (HOMOs) of the sulfur atoms in the thiol groups. These results are similar to conclusions of Ito et al.<sup>23</sup> who performed density-of-states modeling of a related self-assembled thienyl-terminated disulfide, (bis-[2-(3-thienyl)-ethyl]-11,11'-dithiodiundecanate). Note that He I UPS has an even smaller escape depth than XPS performed at a 90° takeoff angle due to the lower kinetic energies of the photoelectrons; the mean free path for 20 eV electrons is 5–10 Å.<sup>51</sup> The strong signal of the low binding energy thiophene valence features supports the conclusions that the thiophene rings extend to the periphery of the assemblies. The small shift of the peak in the range 3.5–3.8 eV, due to the orbitals localized on the thiophene rings, toward higher binding energy in progressing from  $n = 2$  to  $n = 12$  may be due to either

(51) Feldman, L. C.; Mayer, J. W. *Fundamentals of Surface and Thin Film Analysis*; Elsevier Science: New York, 1986; pp 126–130.

**Table 2. Ellipsometric Thickness and Advancing and Receding Contact Angles for Thienyl- and Methyl-Terminated Alkanethiol SAMs on Au(111)**

RSH	molecular length <sup>a</sup> (Å)	observed thickness <sup>b</sup> (Å)	contact angles (deg)			
			$\theta_a(\text{H}_2\text{O})^c$	$\theta_r(\text{H}_2\text{O})^d$	$\Delta\theta(\text{H}_2\text{O})^e$	$\theta_a(\text{HD})^f$
CH <sub>3</sub> (CH <sub>2</sub> ) <sub>2</sub> SH	6.5	5.1	95	79	16	36
CH <sub>3</sub> (CH <sub>2</sub> ) <sub>6</sub> SH	11.6	9.3	110	96	14	38
CH <sub>3</sub> (CH <sub>2</sub> ) <sub>12</sub> SH	19.3	17.2	110	100	10	43
Th(CH <sub>2</sub> ) <sub>2</sub> SH	9.0	6.7	91	68	23	26
Th(CH <sub>2</sub> ) <sub>6</sub> SH	14.1	10.7	90	72	18	25
Th(CH <sub>2</sub> ) <sub>12</sub> SH	21.8	17.9	90	76	14	22

<sup>a</sup> Calculated chain length derived from assumption of a fully extended all-trans conformation using Gaussian 98 at the 6-31G level.

<sup>b</sup> Observed ellipsometric thickness. <sup>c</sup> Advancing water contact angle. <sup>d</sup> Receding water contact angle. <sup>e</sup> Water contact angle hysteresis.

<sup>f</sup> Advancing hexadecane contact angle.

modest differences in the work functions of the samples or small differences in the ionization energies of the orbitals.

**Ellipsometric Thickness Measurements.** The thickness of the thienyl-terminated alkanethiol SAMs was measured using ellipsometry. Table 2 shows the ellipsometric thickness as a function of the number of methylene units. Data for methyl-terminated SAMs having the same number of methylene units are also included. For 2-(3-thienyl)ethanethiol, 6-(3-thienyl)hexanethiol, and 12-(3-thienyl)dodecanethiol monolayers, the ellipsometric values are 6.7, 10.7, and 17.9 Å, respectively. *N*-Alkanethiols with greater than 9 methylene units have been reported to assemble on gold with a tilt angle of 30° from the surface normal, indicating closely packed and well-ordered monolayers.<sup>44</sup> To estimate the tilt angle of the thienyl-terminated SAMs, the theoretical molecular lengths were calculated as the distance between the H in the  $\beta$  position of the thiophene ring and the S on the molecule's other end by assuming that the alkyl chain is in a fully extended all-trans conformation. A value of 1.5 Å was added to account for the distance between the end sulfur of the alkanethiols and the gold substrate.<sup>6</sup> The estimated tilt angles for the thienyl-terminated SAMs are 42°, 41°, and 35° for 2, 6, and 12 methylene units, respectively. Similar calculations for the methyl-terminated SAMs yield tilt angles of 38°, 37°, and 27°, respectively. Ito et al.,<sup>23</sup> who studied the orientational structure of the self-assembled thienyl-terminated disulfide by infrared reflection absorption spectroscopy, reported that the thiophene rings lie almost parallel to the substrate surface, with the alkyl chains tilted slightly from the surface normal. If the thiophene rings in our SAMs adopt a similar geometry, the tilt angles may actually be slightly smaller than the calculated values, since a dihedral angle of 0° was assumed for the thiophene rings with respect to the alkyl chains in calculating the molecular lengths.

**Contact Angle Measurement.** Table 2 contains the results of advancing and receding contact angle measurements for thienyl- and methyl-terminated alkanethiol monolayers using water and hexadecane as the contacting liquids. The measured advancing water contact angles for methyl-terminated monolayers are 95°, 110°, and 110° for 2, 6, and 12 methylene units, respectively. These agree well with reported values.<sup>6,44,52</sup> Bain et al.<sup>6</sup> observed consistent advancing water contact angles of ~110° for *n*-alkanethiol monolayers (CH<sub>3</sub>-(CH<sub>2</sub>)<sub>*n*</sub>-SH) with *n* > 5. However, they noted a marked drop-off in the contact angles when *n* < 5, indicating either that the probe liquid sensed the underlying gold or an increased disorder in short-chain monolayers.

In the case of the thienyl-terminated SAMs, we observe advancing water contact angles of 91°, 90°, and 90° for

methylene unit lengths of 2, 6, and 12, respectively. These lower values relative to those for the methyl-terminated monolayers may be attributed to the thienyl groups located at the periphery of the SAMs, consistent with similarly low advancing water contact angles for *ω*-thiophene-functionalized *n*-alkyltrichlorosilane monolayers.<sup>22,25</sup> Furthermore, Sullivan et al.<sup>22</sup> measured a value of 88° for polythiophene films. Our results suggest that the periphery of the monolayers is comprised of a densely packed array of thiophene groups.

The receding water contact angles for the methyl-terminated alkanethiol monolayers are 79°, 96°, and 100° for 2, 6, and 12 methylene units, respectively. The relatively large contact angle hysteresis values (10°–16°) may result from the surface roughness of the gold substrates on which the SAMs are assembled, consistent with previous reports of increased contact angle hysteresis for gold deposited on chromium/glass substrates relative to thermally annealed gold substrates.<sup>53</sup> In general, gold surfaces prepared by deposition onto annealed substrates (i.e., silicon, mica, glass) show reduced surface roughness and flatter crystallites (~0.2 μm in diameter) than gold substrates prepared by room-temperature deposition.<sup>54</sup> In the present work, we have evaluated the surface roughness of our gold substrates using atomic force microscopy, and this technique reveals crystallites with diameters in the range of 40–60 nm and a valley-to-peak height of 1–3 nm. This roughness likely is the origin of the relatively large water contact angle hysteresis. Note that the thienyl-terminated alkanethiol hystereses are slightly larger than those corresponding to the methyl-terminated SAMs, indicating less homogeneity in the case of the thienyl-terminated monolayers. It is also interesting that the contact angle hysteresis for both the methyl- and thienyl-terminated alkanethiol SAMs decreases as the methylene unit length gets longer, indicating better ordering and higher packing density.

Hexadecane has also been used as a probing liquid. Well-ordered *n*-alkanethiol monolayers have a hexadecane contact angle of 45°,<sup>6,11,44</sup> and when hexadecane contacts only methylene groups, hexadecane completely wets the surfaces (0°).<sup>5,55</sup> We have obtained hexadecane contact angles of 36°, 38°, and 43° for 1-propanethiol, 1-heptanethiol, and 1-tridecanethiol monolayers, respectively. The relatively low contact angles in the case of 1-propanethiol and 1-heptanethiol may arise from the hexadecane contacting the methylene groups, a result of relatively poor packing in the case of the short chains. We observe hexadecane contact angles of 26°, 25°, and 22° for

(53) Kang, J. F.; Ulman, A.; Liao, S.; Jordan, R.; Yang, G.; Liu, G. *Langmuir* **2001**, *17*, 95.

(54) Laibinis, P. E.; Palmer, B. J.; Lee, S.-W.; Jennings, G. K. *Self-Assembled Monolayers of Thiols*; Ulman, A., Ed.; Academic Press: New York, 1998; pp 4–7.

(55) Ferguson, G. S.; Chaudhury, M. K.; Biebuyck, H. A.; Whitesides, G. M. *Macromolecules* **1993**, *26*, 5870.

(52) Troughton, E. B.; Bain, C. D.; Whitesides, G. M.; Nuzzo, R. G.; Allara, D. L.; Porter, M. D. *Langmuir* **1988**, *4*, 365.

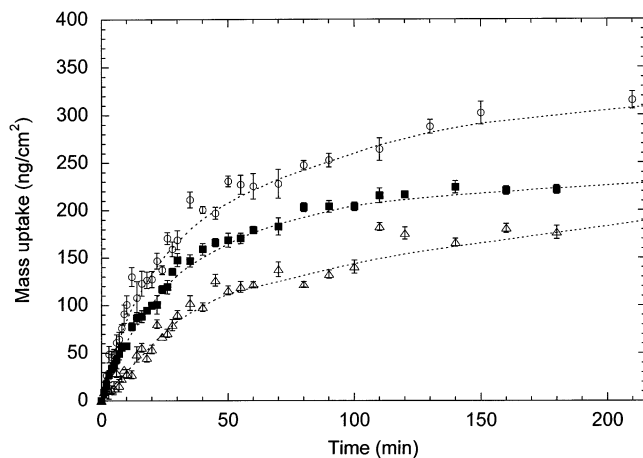


**Figure 8.** Mass uptake change as a function of immersion time of a quartz crystal microbalance in 1 mM 2-(3-thienyl)ethanethiol ( $\Delta$ ), 6-(3-thienyl)hexanethiol ( $\blacksquare$ ), and 12-(3-thienyl)dodecanethiol ( $\circ$ ) solutions. The lines through the data are included to guide the eye. Note that the measurements were performed ex situ, as discussed in the text.

$\text{Th}-(\text{CH}_2)_n-\text{SH}$ , with  $n = 2, 6,$  and  $12$ , respectively. For hexadecane on polythiophene films and thiophene-capped monolayers, contact angles of approximately  $16^\circ$  and  $20^\circ$ , respectively, have been measured.<sup>22</sup> The hexadecane contact angles we observe for thienyl-terminated alkanethiol SAMs are consistent with this value.

**QCM Measurements.** Figure 8 shows mass uptake, converted from ex situ QCM measurements, as a function of immersion time in 1 mM solutions of thienyl-terminated alkanethiols in chloroform. Solution QCM measurements are known to be susceptible to complicating factors,<sup>56</sup> and to verify the performance of the QCM, a test experiment was performed on 1-tridecanethiol. In this case, the equilibrium mass uptake was  $190 \text{ ng/cm}^2$ , corresponding to a packing density of  $5.2 \times 10^{14}$  molecules/ $\text{cm}^2$ , which is in good agreement with the reported value<sup>44</sup> of  $4.7 \times 10^{14}$  molecules/ $\text{cm}^2$ . The equilibrium mass uptake values obtained from the data in Figure 8 are 167, 220, and  $310 \text{ ng/cm}^2$  for 2-(3-thienyl)ethanethiol, 6-(3-thienyl)hexanethiol, and 12-(3-thienyl)dodecanethiol, respectively, corresponding to packing densities of  $6.5, 6.6,$  and  $7.0 \times 10^{14}$  molecules/ $\text{cm}^2$ . These values are larger than for 1-tridecanethiol, indicating greater packing densities in the case of the thiophene-terminated SAMs. This is inconsistent with the conclusions drawn from the ellipsometry data. It is possible that the QCM is overestimating the mass of self-assembled molecules due to physisorbed molecules on top of the SAM layers which are not completely removed by rinsing. This would be expected to be more severe in the case of the thiophene-substituted SAMs because of their longer lengths and increased intermolecular attractions. In any case, we conclude that the thiophene-substituted alkanethiols have comparable packing densities to  $n$ -alkanethiols.

**Thermal Stability Measurements.** Figure 9 shows changes in the XPS C 1s/Au 4f and S 2p/Au 4f ratios as a function of heating temperature. Heating to  $65^\circ\text{C}$  does not significantly change the sulfur intensity but causes a slight decrease in the carbon intensity. This may be due to thermal desorption of small molecules (e.g., CO or  $\text{CO}_2$ ) on the surface of the monolayers. Heating to  $150^\circ\text{C}$  causes dramatic decreases in the C 1s/Au 4f and S 2p/Au 4f ratios. By  $180^\circ\text{C}$ , all of the sulfur has desorbed, but the C 1s/Au 4f ratio is about 0.10, indicating that some carbon remains

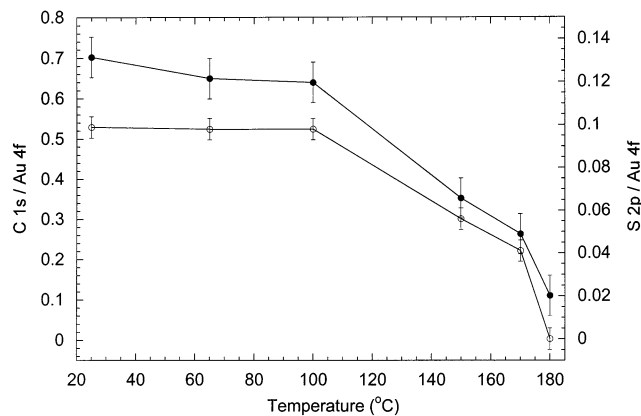


**Figure 9.** Variation in C 1s/Au 4f ratio ( $\bullet$ ) and S 2p/Au 4f ratio ( $\circ$ ) for self-assembled 12-(3-thienyl)dodecanethiol monolayers on Au/Si(111) as a function of heating temperature. The left y-axis refers to the C 1s/Au 4f ratio ( $\bullet$ ); the right one refers to the S 2p/Au 4f ratio ( $\circ$ ).

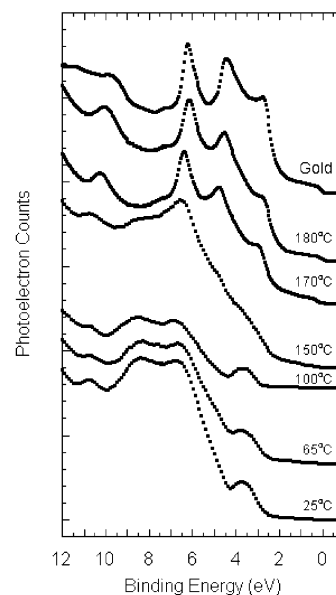


**Figure 10.** He I UPS of self-assembled 12-(3-thienyl)dodecanethiol monolayers on Au/Si(111) as a function of heating temperature. A spectrum of clean gold is included for reference.

on the surface. This residual carbon may have its origin in thermal decomposition of the SAM to carbon-containing species that remain on the surface.

Figure 10 shows He I UPS spectra for the heating of self-assembled 12-(3-thienyl)dodecanethiol. A spectrum of clean gold (argon ion sputtered to remove any contaminants) is also included for reference. As discussed previously, the peak at  $3.8 \text{ eV}$  is mainly due to localized thiophene ring electronic states with some contributions from the thiol sulfur atoms. This peak persists to temperatures as high as  $100^\circ\text{C}$ ; by  $150^\circ\text{C}$  it has essentially disappeared. This result is consistent with conclusions drawn from the XPS data. The UPS spectrum after heating to  $180^\circ\text{C}$  shows features characteristic of bulk gold, indicating desorption of the monolayers.  $N$ -Alkanethiol SAMs are reportedly thermally stable in vacuum up to approximately  $100^\circ\text{C}$ ; heating to ca.  $200^\circ\text{C}$  leads to monolayer desorption.<sup>57–59</sup> Our results indicate that the thienyl-terminated SAMs behave similarly.

(57) Poirier, G. E.; Tarlov, M. J.; Rushmeier, H. E. *Langmuir* **1994**, *10*, 3383.

(58) Li, J.; Liang, K. S.; Camillone, N.; Leung, T. Y. B.; Scoles, G. J. *Chem. Phys.* **1995**, *102*, 5012.

(56) Karpovich, D. S.; Blanchard, G. J. *Langmuir* **1994**, *10*, 3315.

### Conclusions

Thiophene-containing alkanethiols, Th-(CH<sub>2</sub>)<sub>n</sub>-SH (Th = 3-thiophene) with  $n=2, 6,$  and  $12,$  have been synthesized and self-assembled onto Au(111) surfaces. The properties of these monolayers have been compared with those of methyl-terminated SAMs having the same number of methylene units. Adsorption of the thiols via formation of a surface thiolate bond is demonstrated by angle-resolved XPS measurements and UPS. Contact angle measurements also indicate that the thiophene functional group is at the periphery of the monolayer. Ellipsometry and QCM measurements show that 12-(3-thienyl)do-

decanethiol forms well-ordered and closely packed monolayers on gold, exhibiting a tilt angle of 35°. 2-(3-Thienyl)ethanethiol and 6-(3-thienyl)hexanethiol form less packed monolayers and have greater tilt angles of 42° and 41°, apparently caused by disordering of the shorter alkyl chains.

**Acknowledgment.** This material is based upon work supported by the National Science Foundation under Grant No. DMR-0089960. Insightful discussions with Professor Jayant Kumar and Dr. Dongwook Kim are acknowledged. M. Kim thanks the Council for Federated Centers and Institutes at the University of Massachusetts Lowell for a research assistantship.

---

(59) McCarley, R. L.; Dunaway, D. J.; Willicut, R. J. *Langmuir* **1993**, *9*, 2775.

LA0208979